Simulation of pressurizer water level and causes of false water level in marine conditions

YANG Bo[1], XIA Hong[2], and ZHANG Ji-yu[3]

1. College of Nuclear Science and Technology, HARBIN ENGINEERING UNIVERSITY, No.145 Nantong Street, Harbin, Heilongjiang Province, 150000, P.R. China (yangbo12345@126.com)
2. College of Nuclear Science and Technology, HARBIN ENGINEERING UNIVERSITY, No.145 Nantong Street, Harbin, Heilongjiang Province, 150000, P.R. China (xiahong@hrbeu.edu.cn)
3. College of Nuclear Science and Technology, HARBIN ENGINEERING UNIVERSITY, No.145 Nantong Street, Harbin, Heilongjiang Province, 150000, P.R. China (82134227@qq.com)

Abstract: For marine nuclear reactors, the pressurizer is the key equipment for controlling the pressure stability of the reactor coolant system. One of the major problems in its design process is the liquid sloshing in the tank. In the study of liquid sloshing on the water level measurement in the pressurizer under marine conditions, it was verified that the SPH (Smoothed Particle Hydrodynamics) method can simulate the free liquid surface during sloshing well, and used to simulate the sloshing effects on the free liquid surface in the "Mutsu"'s pressurizer under marine conditions. In this paper, the effects of sloshing on 6 degrees of freedom (6-DOF) on the liquid level measurement were analyzed and compared with the experimental results, and they were in good agreement. Simultaneously, the cause of the false liquid level was analyzed by comparing the measured point pressure with the simulated water level. The analysis result shows that the vertical acceleration is the main cause of false liquid level, and the relationship between them is linear. According to the cause of the false water level, the compensation design of the pressurizer water level measurement was given. This study provides a reference for the design of pressurizer water level measurement system under marine conditions.
Keyword: pressurizer; SPH; water level; sloshing

1 Introduction

The pressurizer is a key equipment for controlling the pressure stability of the reactor coolant system, a major problem in its design process is liquid sloshing. The phenomenon of liquid sloshing is strong non-linear. The sloshing motion depends on various factors, such as the container's movement, liquid-filled depth, liquid properties, and the container's geometry [1]. The false liquid level due to the sloshing may cause false alarms and other problems. It can directly affect the safety of personnel and equipment. Therefore, it is necessary to study the sloshing characteristics of the pressurizer to reduce the influence of sloshing on each device of the nuclear power plant and improve the safety of the marine nuclear power plant.

To study the complex liquid sloshing properties, numerical simulation needs to be conducted. Common numerical simulation methods include finite difference method, finite element method and boundary element method. These conventional mesh-based methods have difficulties in handling large deformations of free surfaces, over-distorted mesh, and crushing waves. Therefore, the meshless methods were used well in dealing with such problems in recent years. As one of the meshless methods, SPH has a great advantage that when using it to deal with sloshing problems of liquids, information such as motion history, free liquid surface, and moving boundary can be directly obtained. Therefore, SPH is widely used in the problems such as dam breaks, explosions and free surface flow.

In the study of the pressurizer's water level change under marine conditions, Toshihisa ISHIDA used the RETRAN-02/GRAV program to analyze the experimental data of the "Mutsu" in the time domain and frequency domain. It was found that the vertical acceleration had the greatest influence on the water level changes of the steam generator and the pressurizer [2]. To further study the characteristics of the water level change of the pressurizer under marine conditions, the 6-DOF motion response of waves and ships were calculated and simulated. At the same time, the SPH method was used to simulate the water level

Received date: November 11, 2018
(Revised date: January 10, 2019)

measurement of the pressurizer under marine conditions. The pressure of the measuring point inside the pressurizer was simulated under the experimental conditions of the "Mutsu", and the main parameters affecting the water level measurement were analyzed. It provided reference for improving the water level measurement system of the pressurizer under the marine conditions.

2 SPH basic principles

The method of studying the sloshing problem can be summarized into three methods: analytical method, experimental method and numerical method. Analytical method has limitations due to the randomness and high nonlinearity of the sloshing problems. Many problems are still not solved well and require a lot of research work [3]. The experimental method is the most reliable way to study sloshing problems. However, it is usually needs high costs and long test cycles. The numerical method can make up for the deficiency of the former and the simulation accuracy of the physical phenomenon is also high. Therefore, the numerical method has become one of the main methods to study the sloshing problem.

Since the sloshing problem was discovered in engineering, researchers have obtained a lot of results on the sloshing problem and formed some effective research methods. Cui Yan [4] used the SPH method to study the variation of the wave height of a two-dimensional rectangular tank near the resonance frequency in the longitudinal oscillation. Anghiler [5] used the finite element method, pure Euler method, arbitrary Euler-Lagrange method, and SPH method to perform numerical calculations on the hydrodynamic loading at the bottom of the tank. Comparing the results of the four methods, it was found that the SPH method has advantages in simulating the complex forms of liquid sloshing. The following parts will introduce the basic principles of the SPH method.

2.1 SPH's key ideas

(1) The problem domain is represented by a series of randomly distributed particles.

(2) The integral representation is used to approximate the field function. Then the integral expression of $f(x)$ can be written as:

$$f(x)=\int_{\Omega} f(x')W(x-x',h)dx' \tag{1}$$

(3) Particles are used to further approximate the kernel approximation equation. The particle approximation of the function at particle i can eventually be written as:

$$f(x_i)=\sum_{j=1}^{N}\frac{m_j}{\rho_j}f(x_j)\cdot W(x_i-x_j,h) \tag{2}$$

In the formula, ρ_j is the density of particle *j*. *h* is the smooth length of the affected area of the smooth function *W*.

(4) The particle approximation process is performed within each time step to determine the support domain again. Therefore, the SPH method is adaptive.

(5) The particle approximation method is applied to the field function related terms of all partial differential equations to obtain a series of discretized time-dependent ordinary differential equations.

(6) Apply the explicit method to solve ordinary differential equations to obtain the fastest time integral and the variation over time of all particle field variables.

2.2 Construction of a smooth function

Since smooth functions determine the accuracy of the function expression and the computational efficiency, the construction of the smooth function plays a crucial role in the SPH method. So far, there are many examples of constructing smooth functions in related literature on the SPH method, and now summarize all the main characteristics of the smooth function as follows:

(1) The smoothing function must be normalized over its support domain (Unity)

$$\int_{\Omega} W(x-x',h)dx'=1 \tag{3}$$

This normalization property ensures that the integral of the smoothing function over the support domain to be unity.

(2) The smoothing function should be compactly supported (Compact support), *i.e.*

$$W(x-x')=0, |x-x'|>\kappa h \tag{4}$$

The dimension of the compact support is defined by the smoothing length h and a scaling factor κ, where h is the smoothing length, and κ determines the spread of the specified smoothing function. $|x-x'|>\kappa h$ defines the support domain of the particle at point x.

(3) $W(x-x')\geq 0$ for any point at x within the support domain of the particle at point x (Non-negativity). This property states that the smoothing function should be non-negative in the support domain.

(4) The smoothing function value for a particle should be monotonically decreasing with the increase of the distance away from the particle (Decay).

(5) The smoothing function should satisfy the Dirac delta function condition as the smoothing length approaches zero (Delta function property)

$$\lim_{h\to 0} W(x-x',h)=\delta(x-x') \tag{5}$$

This property makes sure that as the smoothing length tends to be zero, the approximation value approaches the function value, *i.e.* $\langle f(x)\rangle = f(x)$.

(6) The smoothing function should be an even function (Symmetric property). This means that particles from same distance but different positions should have equal effect on a given particle.

(7) The smoothing function should be sufficiently smooth (Smoothness). This property aims to obtain better approximation accuracy. For the approximations of a function and its derivatives, a smoothing function needs to be sufficiently continuous to obtain good results. A smoothing function with smoother value of the function and derivatives would usually yield better results and better performance in numerical stability.

2.3 Particles approximation of N-S equation by SPH method

Using the afore-mentioned kernel and particle approximation techniques with necessary numerical tricks, it is possible to derive SPH formulations for partial differential equations governing the physics of fluid flows. For Navier-Stokes equations controlling the general fluid dynamic problems, we use α and β to represent the coordinate direction and use the index method to represent the superposition of equations. We have

(1) Continuity equation:

$$\frac{d\rho_i}{dt}=\sum_{j=1}^{N} m_j v_{ij}^{\beta}\frac{\partial W_{ij}}{\partial x_i^{\beta}} \tag{6}$$

(2) Momentum equation:

$$\frac{dv_i^{\alpha}}{dt}=\sum_{j=1}^{N} m_j \frac{\sigma_i^{\alpha\beta}+\sigma_j^{\alpha\beta}}{\rho_i\rho_j}\frac{\partial W_{ij}}{\partial x_i^{\beta}} \tag{7}$$

(3) Energy equation:

$$\frac{de_i}{dt}=\frac{1}{2}\sum_{j=1}^{N} m_j \frac{\rho_i+\rho_j}{\rho_i\rho_j} v_{ij}^{\beta}\frac{\partial W_{ij}}{\partial x_i^{\beta}}+\frac{\mu_i}{2\rho_i}\varepsilon_i^{\alpha\beta}\varepsilon_j^{\alpha\beta} \tag{8}$$

where

$$v_{ij}^{\beta}=(v_i^{\beta}-v_j^{\beta}) \tag{9}$$

In the above formula, α and β represent the coordinate direction. σ is composed of the total stress tensor p and the viscous stress τ.

$$\varepsilon^{\alpha\beta}=\frac{\partial v^{\beta}}{\partial v^{\alpha}}+\frac{\partial v^{\alpha}}{\partial x^{\beta}}-\frac{2}{3}(\nabla\cdot v)\delta^{\alpha\beta} \tag{10}$$

Specific formula derivation process refers to the monograph [6].

2.4 Artificial viscosity

To simulate the fluid dynamics problem and prevent the non-physical oscillation of the solution results, artificial viscosity needs to be used in the simulation to ensure the stability of the calculation. Till now, Monaghan's artificial viscosity [7] has been used most extensively. The specific expressions are as follows:

$$\Pi_{ij}=\begin{cases}\dfrac{-\alpha_{\Pi}\bar{c}_{ij}\phi_{ij}+\beta_{\Pi}\phi_{ij}^2}{\bar{\rho}_{ij}}, & v_{ij}\cdot x_{ij}<0\\ 0, & v_{ij}\cdot x_{ij}\geq 0\end{cases} \tag{11}$$

where

$$\phi_{ij}=\frac{h_{ij}v_{ij}\cdot x_{ij}}{|x_{ij}|^2+\varphi^2};\qquad \bar{c}_{ij}=\frac{1}{2}(c_i+c_j) \tag{12}$$

$$\bar{\rho}_{ij} = \frac{1}{2}(\rho_i + \rho_j); \qquad h_{ij} = \frac{1}{2}(h_i + h_j) \tag{13}$$

$$v_{ij} = v_i - v_j, \qquad x_{ij} = x_i - x_j \tag{14}$$

In the above equations, α_Π and β_Π are standard constants, generally about 1.0. φ=0.1h_{ij} is used to prevent numerical divergence when particles are close to each other. *c* and *v* represent the speed of sound and the speed of the particles, respectively.

2.5 Boundary processing

For free surface boundaries, the SPH method can be naturally satisfied. For the boundary of the solid wall, the boundaries of the particles near the boundary will be truncated when SPH integration occurs. This makes the gradient calculation of the variables near the boundary incorrect, so we use two types of virtual particles simultaneously for processing. The first type is an edge wall virtual particle that distributes on the side wall and acts as a strong repulsive force on the inner solid particles that are too close to the side wall to prevent non-physical penetration. The second type is a mirrored virtual particle. For a real particle whose distance to the side wall is less than 1, a particle is disposed symmetrically with the real particle outside the boundary and has the same density, pressure, and smooth length as the corresponding real particle. They have the same speed, but in the opposite direction.

3 SPH feasibility verification

3.1 Benchmark experimental model

In this paper, a set of experiments conducted by the Model Basin Research Group (CEHINAV), the Naval Architecture Department (ETSIN), and the Technical University of Madrid (UPM) at the Technical University of Madrid in 2012, was selected as the benchmark experiment [8]. This set of experiments was used to verify the feasibility of the SPH method applied to liquid sloshing problems.

In this experiment, the rigid rectangular tank model was made of organic glass plates, and the internal dimensions of the model were 900**mm**×62**mm**×508**mm** (length×width×height). The selected liquid was clean tap water at room temperature, the water level was 0.093**m**, and a green fluorescence dye was added to the water. The pressure sensor was placed on the left side wall, 0.093**m** away from the bottom. The specific layout of the tank was shown in Fig.1. The actual photo was shown in Fig.2.

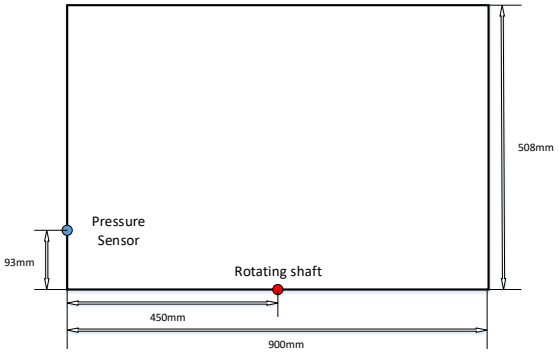

Fig.1 Experimental tank model.

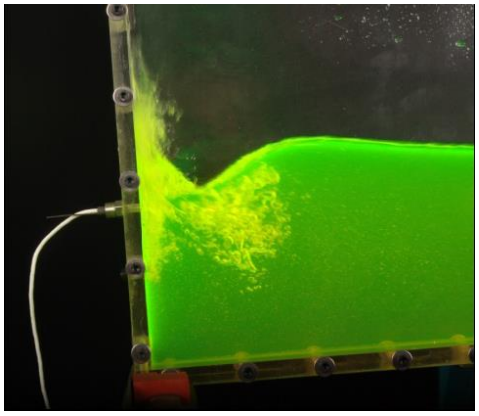

Fig.2 Material object pressure measurement point position.

3.2 Benchmark numerical model

The distribution of the model and pressure measurement points in the numerical calculation were consistent with those in the benchmark experiment. The liquid density was 1000**kg/m³**, and the Monaghan-type artificial viscosity was used for fluid calculation. Particle spacing was 0.005**m**. Initial particle speed was 0**m/s**. Gravity acceleration was 9.8**m/s²**. Initial smooth length was 0.008**m**. Initial calculation time step was 0.0001**s**. Minimum calculation time step was 0.00001**s**. Output time step was 0.01**s**.

Because of the force exerted by the boundary particles on the fluid particles creates a small gap between them, the pressure measurement points placed in the gap will less than the actual number of fluid particles and produce erroneous results. To avoid this problem, it is recommended to place the

pressure measurement point at 1.5 times of the smooth radius from the boundary position.

3.3 Simulation conditions

In the liquid sloshing experiment, the pitch excitation signal designed in this paper was $\theta = A\sin(2\pi ft)$, where A and f were the excitation amplitude and frequency. $A = 4°, f = 0.6137\text{Hz}$. At the initial moment, the tank was in a horizontal position and the axis of rotation was at the center line of the bottom of the tank. Because the experimental stage cannot be directly moved by this angular displacement during the initial stage, the actual angular displacement curve was shown in Fig.3.

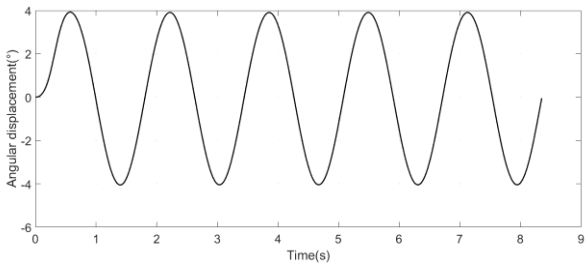

Fig.3 Water tank actual angular displacement.

3.4 Benchmark experiment results

The above constructed numerical model and the given parameters were submitted to the open source software DualSPHysics for parallel calculation, and the free liquid surface shape during the four swing cycles under pitch excitation can be obtained, as shown in Fig.4.

For a clearer presentation, instead of using a three-dimensional perspective, the xOz plane was taken as the viewing plane. As can be seen from the figure ( ), the SPH method can capture the movement of the free liquid surface well when simulating the fluid flow in the tank. And it also can accurately simulate the highly nonlinear state of the liquid level such as the hydraulic jump and the breaking waves.

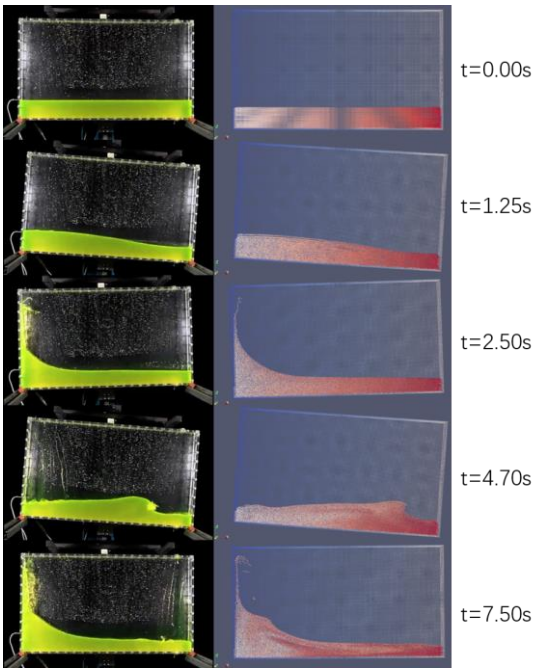

Fig.4 Benchmark experiment typical time free surface.

In addition, the measuring point pressure values obtained in the simulation are compared with the experimental values, as shown in Fig.5. It can be found that there was a slight phase difference between the two curves, and the simulation results were on average about 0.05**s** earlier than the experimental results and can be ignored. The pressure amplitude and peak interval at the key points of the two curves were basically the same. Therefore, it can be considered that the SPH method can realistically simulate the physical phenomena in liquid sloshing.

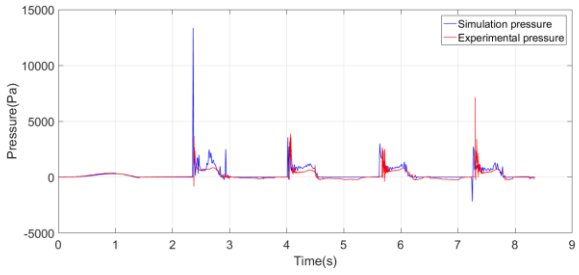

Fig.5 Benchmark experiment point pressure comparison.

4 Simulation of liquid sloshing in pressurizer under marine conditions

4.1 Pressurizer model

The pressurizer is welded by the upper and lower heads and the cylindrical body. The upper part is the steam space and the lower part is the water space.

The pressurizer includes four major components: spray system, electric heater, safety valve group and measuring instrument. Among them, the spray system is in the gas phase space of the pressurizer, the safety valve group and the measuring instrument are all arranged near the side wall of the pressurizer, and only the electric heater is in the liquid phase space. The electric heater occupied less volume in the pressurizer and has less influence on the liquid sloshing. Therefore, the pressurizer can be approximated as a hollow cylindrical cavity during modeling.

When creating the pressurizer model, the following simplifications and assumptions were made:

(1) The pressure in the pressurizer does not affect the sloshing of the liquid;
(2) The effect of liquid temperature on the viscosity of the pressurizer is negligible;
(3) The pressurizer is approximated as a hollow cylindrical cavity;
(4) Assume that the regulator is rigid;
(5) Considering that the amount of calculation is too large, the three-dimensional cylindrical cavity was converted into two-dimensional model.

Based on the above simplifications and assumptions, the pressurizer model was established. The pressurizer model has a diameter of 0.5**m**, a height of 3**m** and a particle spacing of 0.002**m**. There are 3,500 border particles in this model. The model and the Mutsu's pressurizer meet the model similarity rule in geometry, motion, dynamics, boundary conditions and initial conditions.

4.2 Simulation of wave and ship motion response

Under marine conditions, the essential research on the movement of marine nuclear power plants is to simulate the motion response of ships. In this paper, the waves were simulated first, and then the loads received by the ship in the waves were analyzed. Furthermore, we can calculate the ship's motion response in 6-DOF. In fact, it is difficult to accurately model and describe the waves. Because of this process is nonlinear and strongly random, therefore, when we selected the method for simulating ocean waves, we referred to the relevant literature [12] and decided to use wave spectrum theory to model the waves.

Long-term observations and studies have shown that waves are generalized stationary random processes and have ergodicity. Describe the waves distribution from the whole process is more profound and more practical than simply describing. The wave spectrum is the distribution of the energy in the frequency domain during the steady state of the waves, it reflects the internal structure of the waves, and the relationship between the amplitude and wave frequency. In the actual use, various research institutes have established different wave spectra for different ocean areas and conditions. As of the subject of this study was an experiment on the Atlantic Ocean by Japan's Mutsu, the ITTC two-parameter spectrum[13] was used to simulate the waves after analyzing and comparing different wave spectra. The expression is as follows:

$$S_{\varsigma}(\omega)=\frac{173H_{1/3}^{2}}{T_{1}^{4}\omega^{5}}\exp(-\frac{691}{T_{1}^{4}\omega^{4}})\ \ (m^{2}\cdot s) \qquad (15)$$

In the formula, $H_{1/3}$ indicates significant ocean wave heights and T_1 indicates the characteristic period of the ocean wave.

The effective wave height was 5**m** and the period was 8**s**. The time-domain and frequency-domain responses of the 6-DOF waves of 0-100**s** are simulated by Matlab, as shown in Fig.6 and Fig.7.

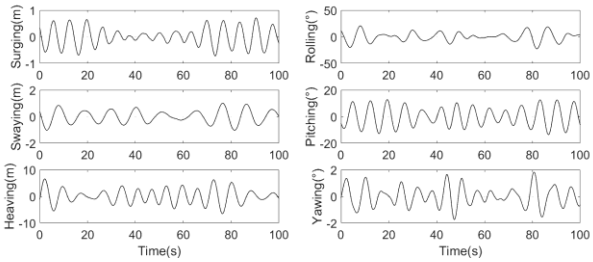

Fig.6 Time domain response on six degrees of freedom of waves.

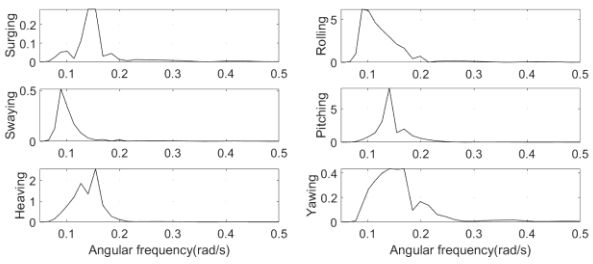

Fig.7 Frequency domain response on six degrees of freedom of waves.

According to related theories, the ship's motion in the waves is strongly non-linear. In this paper, the frequency domain analysis method of potential flow theory was used. According to the design parameters of Mutsu, a simplified model of "Mutsu" below the waterline was established in 3DMAX. The model has a total weight of 8,240 tons. The length, width and height were 130m, 19m and 6.9m respectively. The model was imported into AQWA, a commercial calculation software ANSYS, and the 6-DOF motion response of Mutsu was calculated using the finite element method under the condition of 15 knots and heading angle of 45 degrees. The time domain response is shown in Fig.8, and the frequency domain response is shown in Fig.9.

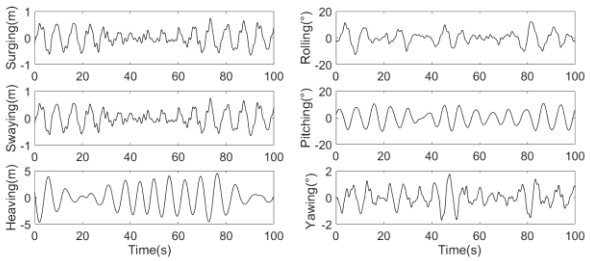

Fig.8 Time domain response on six degrees of freedom of Mutsu.

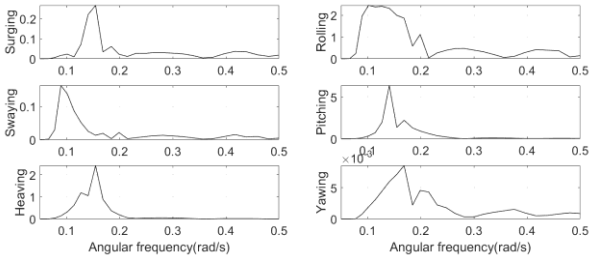

Fig.9 Frequency domain response on six degrees of freedom of Mutsu.

4.3 Initial conditions and particle modeling

Because of the gas-liquid space ratio in the pressurizer is 2:3, so the liquid level is 1.8**m**. When the pressurizer is operating at full power, the absolute pressure is 15.5**MPa** and the corresponding saturation temperature is 344 ℃. At this temperature, the saturated water density at this pressure is 593.95**kg/m^3**. Monaghan type artificial viscosity was used for fluid calculation, the simulation time was 0-25**s**, the fluid particle spacing was 0.002**m**, the total particle number was 225000, the initial velocity was 0**m/s**, the initial smooth length was 0.0032**m**, and the global gravity acceleration was 9.8**m/s^2**. The initial calculation time, minimum calculation time step, and output result time step were 0.0001**s**, 0.00001**s**, and 0.01**s**, respectively. As of the pressure measurement points should be arranged at 1.5 times the smooth radius from the boundary position, the pressure recording point was arranged at the position shown in Fig.10 during the simulation.

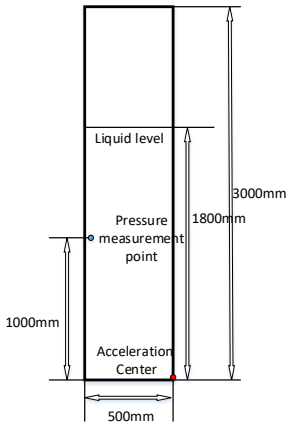

Fig.10 Pressurizer model.

4.4 Analysis of simulation results

In the calculation, we can equate the movement of the tank as a change in the acceleration of gravity. Specifically, for experimental conditions, the tank performs a simple harmonic rotation while the gravity vector is constant. For the simulation case, it was equivalent to the fact that the water tank was not moving, and the gravity vector did simple harmonic rotation. We can decompose the gravity vector into the x and z directions so that the motion represented by the displacement can be reduced to a motion represented by an acceleration of 6-DOF.

Since the pressurizer was almost at the center of "Mutsu", it can be assumed that the motion response of "Mutsu" 6-DOF coincides with the motion of the pressurizer. Therefore, when we numerically simulate the pressurizer sloshing in the ocean, we can decompose the 6-DOF motion of Mutsu into the x-direction line acceleration, the z-direction line acceleration and the y-direction angular acceleration. During 0-25**s**, the transformed three-degree-of-freedom motion responses the curve of Mutsu as shown in Fig.11.

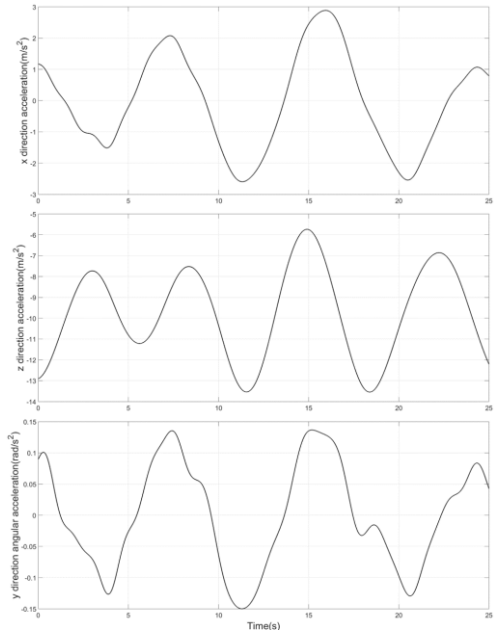

Fig.11 Transformed three-degree-of-freedom motion response curve of Mutsu.

The pressure in the pressurizer under full power steady state conditions was 15.5**MPa**, but no initial pressure was set during the simulation. Therefore, the pressure value obtained by the simulation did not reflect the true pressure in the pressurizer, so the normalization processing was necessary to be carried out. Figure 12 shows the pressure values of the measurement points obtained after the normalization process. There was a numerical oscillation in the first half of the curve, so the only pressure changes in the second half were analyzed.

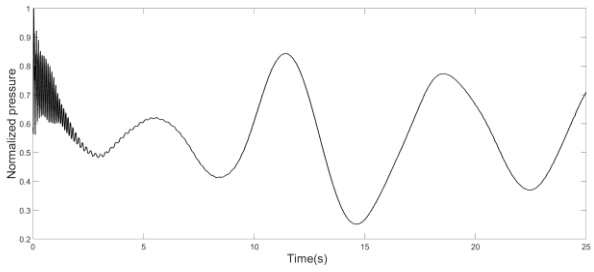

Fig.12 0-25s simulation point pressure change.

By comparing the motion response in Fig.11 with the pressure value in Fig.12, it can be concluded that the pressure change trends at the measuring point is the same as the trend of the vertical acceleration, and the peak time of the two is almost the same. This shows that the change of water level is strongly influenced by vertical acceleration. The pressure at the measuring point has no obvious relationship with the other two accelerations. These conclusions are consistent with the experimental results of Mutsu.

Under the boundary conditions above and initial conditions, simulation results of the free liquid surface shape simulation are shown in Fig.13. During the entire simulation process, there was no strong non-linear phenomenon such as curling and splashing on the free liquid surface, so there was no large impact on the pressurizer.

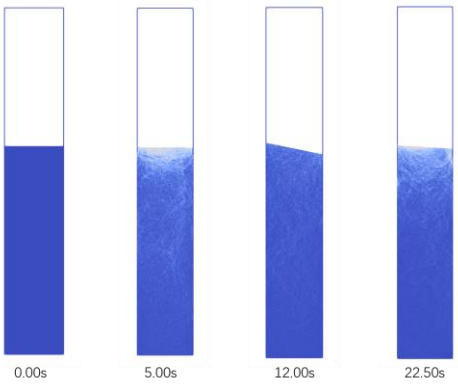

Fig.13 Pressurizer free liquid surface at typical time.

5 Conclusions

In this paper, the SPH method was used to simulate the water level change characteristics of the pressurizer under marine conditions. By comparing with the benchmark experiment and the actual operation data of Mutsu, it is proved that the SPH method can be well applied to the research of sloshing problem. The research results show that the waves that effect on the pressurizer water level measurement under marine conditions are mainly low-frequency waves, and there is no large fluctuation in the free liquid level of the pressurizer water level in this frequency. However, the current solution for measuring the water level of the pressurizer is the static pressure measurement, so the pressure value at the measurement point will change with the change of the vertical acceleration. Thereby it will affect the level of measured values. By analyzing the acceleration in the vertical direction and the pressure at the measuring point, a linear relationship between the measured water level and the acceleration in the vertical direction is found.

Based on the analysis of the characteristics of the water level of the pressurizer under marine conditions,

we propose two proposals for improving the water level measurement system.

(1) Increase the accuracy of the three-axis acceleration sensor and substitute the measured acceleration into the water level change relation to compensate for the water level measurement.
(2) Research on a new water level sensor to directly detect the position of the free liquid surface.

Acknowledgement

This study was partially supported by the Natural Science Foundation of China (Grant No. 51379046) and the Natural Science Foundation of Heilongjiang Province. China (Grant No. E2017023), which are gratefully acknowledged. The authors also thank the open-resource SPH Solver (http://www.dual.sphysics.org/) for its valuable reference.

References

[1] DE-ZHI, N., WEI-HUA, S., and BIN, T.: Nonlinear numerical simulation of liquid sloshing in a container subjected to pitch excitation[J]. Journal of Ship Mechanics, 2017, 21(1):15-22.
[2] ISHIDA, T., KUSUNOKI, T., and IOCHIAI, M., *et al.*: Effects by Sea Wave on Thermal Hydraulics of Marine Reactor System[J]. Journal of Nuclear Science and Technology, 1995, 32(8):12.
[3] CAI, Z.H.: Study on The Sloshing Problems of Liquid Cargo Tanks[D]. Shanghai Jiao Tong University, 2012.
[4] CUI, Y.: Numerical Simulation of Sloshing in Two Dimensional Rectangular Tanks with SPH[D]. Shanghai Jiao Tong University, 2008.
[5] ANGHILERI, M., CASTELLETTI, L.M.L., and TIRELLI, M.: Fluid–structure interaction of water filled tanks during the impact with the ground[J]. International Journal of Impact Engineering, 2005, 31(3):235-254.
[6] LIU, M.B., and LIU, G.R.: Smoothed Particle Hydrodynamics (SPH): An Overview and Recent Developments[J]. Archives of Computational Methods in Engineering, 2010, 17(1):25-76.
[7] MONAGHAN, J.J.: An introduction to SPH[J]. Computer Physics Communications, 1988, 48(1):89-96.
[8] DELORME, L., COLAGROSSI, A., and SOUTOIGLESIAS, A., *et al.*: A set of canonical problems in sloshing, Part I: Pressure field in forced roll-comparison between experimental results and SPH[J]. Ocean Engineering, 2009, 36(2):168-178.
[9] SOUTO-IGLESIAS, A., BOTIA-VERA, E., and MARTÍN, A., *et al.*: A set of canonical problems in sloshing. Part 0: Experimental setup and data processing[J]. Ocean Engineering, 2011, 38(16):1823-1830.
[10] SOUTO-IGLESIAS, A., BOTIA-VERA, E., and BULIAN, G.: Repeatability and Two-Dimensionality of model scale sloshing impacts[C]. In International Offshore and Polar Engineering Conference (ISOPE), 2011.
[11] BOTIA-VERA, E., SOUTO-IGLESIAS, A., BULIAN, G., and LOBOVSKÝ, L.: Three SPH Novel Benchmark Test Cases for free surface flows[C]. In 5th ERCOFTAC SPHERIC workshop on SPH applications, 2010.
[12] HE, L.S.: A Study on The Dynamic Response of Ultra Large Ships in Waves[D]. Wuhan University of Technology, 2013.
[13] WANG, X.L.: Study on Wave-induce Motion of the Large Derrick Barge Ships[D]. Tianjin University, 2003.